Electron performance with the ATLAS detector with J/ψ, W and Z

Nicolas Kerschen for the ATLAS Collaboration
CERN, CH-1211 Genève 23, Switzerland

DOI: http://dx.doi.org/10.3204/DESY-PROC-2010-01/215

We outline the electron performance of the ATLAS detector with the very first data taken at the LHC with a center of mass energy of 7 TeV. In particular, the first observation of J/ψ in the electron channel is shown as well as the first Monte-Carlo/Data comparisons of the main variables used in electron identification. Good agreement is demonstrated between observation and expectation for electron reconstruction and identification. An brief outlook on future studies to extract the electron efficiency and the calorimeter energy scale and uniformity of response using J/ψ, W and Z is also given.

1 Introduction

The electron reconstruction and identification algorithms used in ATLAS are designed to achieve both a large background rejection and a high and uniform efficiency over the full acceptance of the detector for transverse energies above 20 GeV. Isolated electrons need to be separated from hadrons in jets, from background electrons (originating mostly from photon conversions in the tracker material), and from non-isolated electrons from heavy flavour decays. The main subdetectors involved in the identification of electrons are the ATLAS electromagnetic (EM) calorimeter and the ATLAS inner detector. The ATLAS detector is described elsewhere [1]. The EM calorimeter has a fine lateral segmentation and three layers in the longitudinal direction of the showers complemented by a presampler placed in front. At high energy, most of the EM shower energy is collected in the second layer which has a lateral granularity of 0.025×0.025 in $\eta \times \phi$ space. The first layer consists of finer-grained strips in η. The fine lateral granularity extends up to $|\eta| < 2.47$. The calorimeter is divided into a barrel part and two end-caps with an overlapping region in $1.37 < |\eta| < 1.52$. The ATLAS inner detector provides precise track reconstruction over $|\eta| < 2.5$. It consists of three layers of pixel detectors close to the beam-pipe, 8 layers of silicon microstrip detectors (SCT) providing 4 space points per track at intermediate radii, and a transition radiation tracker (TRT) at the outer radii, providing about 35 hits per track (in the range $|\eta| < 2.0$). The TRT also provides substantial discriminating power between electrons and pions over a wide energy range (between 0.5 and 100 GeV). The pixel vertexing layer (also called the B-layer) is located just outside the beam-pipe at a radius of 50 mm, and provides precision vertexing and significant rejection of photon conversions (through a requirement of a track with a hit in this layer).

2 Electron reconstruction

Electron reconstruction begins with the creation of a preliminary set of clusters in the EM calorimeter. The size of these seed clusters corresponds to 3×5 cells in $\eta \times \phi$, in the middle layer of the EM calorimeter. Electron reconstruction is seeded from such clusters with $E_T > 2.5$ GeV using a sliding window algorithm over the full acceptance of the EM calorimeter. Electrons are reconstructed from the sliding window clusters if there is a suitable match with a track of $p_T > 0.5$ GeV. The "best" track is the one lying with an extrapolation closest in (η, ϕ) to the cluster barycentre in the middle EM calorimeter layer. For the barrel EM calorimeter, the optimal cluster size for electron candidates is 3×7 cells in $\eta \times \phi$, whereas it is 5×5 cells for the end-cap EM calorimeters. The cluster energy is calibrated with simulated events by parametrising, in fine η bins, the energy lost by the electron along its path as a function of the measured energy in the cluster. Figure 1 shows the linearity of the response of the EM calorimeter in simulated events, defined as the ratio between the reconstructed and the true electron energy as a function of pseudorapidity and at different energies. The deviation from linearity is less than 0.5 % at almost all values of $|\eta|$. The fractional energy resolution σ/E as a function of $|\eta|$ is shown in Fig. 1 for different energies. First studies on low energy photons from neutral pion decays indicate an overall uniformity in η better than 2 % and a unformity in ϕ better than 0.7 % for the barrel and end-cap calorimeters.

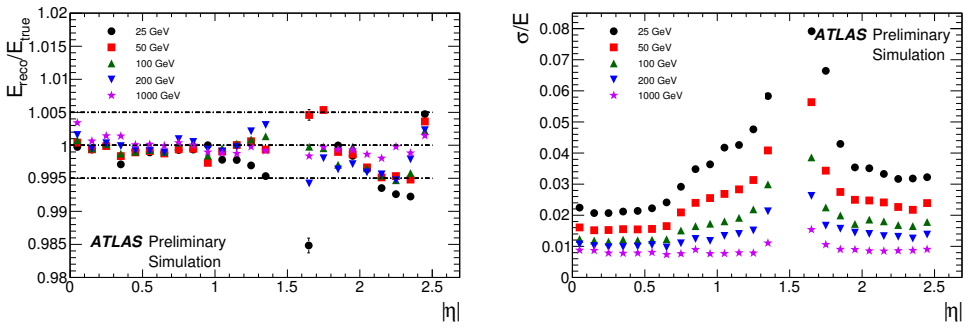

Figure 1: Linearity (left) and Resolution (right) of the EM calorimeter.

3 Electron identification

The baseline electron identification algorithms in ATLAS rely on rectangular cuts using variables which deliver good separation between isolated electrons and fake signatures from jets. These variables include calorimeter, tracker, and combined calorimeter/tracker information. Three reference sets of cuts have been defined for electrons: loose, medium, and tight. The cut values are optimised in bins of E_T and $|\eta|$. Shower shape variables of the second calorimeter layer and hadronic leakage variables are used in the loose selection. Strip cuts, track quality requirements, and track-cluster matching are added at the level of the medium selection. The tight selection adds E/p, B-layer hit requirements, and the particle identification potential of the TRT. For robustness, cut choices (including thresholds) are based on the expected level of

understanding of the detector performance at start-up.

Figure 2 shows the shower shapes for a selection of electron candidates corresponding to 1 nb^{-1} of integrated luminosity. The preselection cuts applied are: transverse energy of the cluster greater than 5 GeV, $|\eta| < 2.0$ (excluding the EM calorimeter barrel/end-caps overlapping region), number of silicon hits greater than 4 and number of TRT hits greater than 10. The shapes shown in Fig. 2 correspond to the discriminating variables used in the loose electron selection. These are: the longitudinal shower leakage (ratio of E_T in the hadronic calorimeter to E_T of the EM cluster), the ratio of cell energies in 3×7 versus 7×7 cells in $\eta \times \phi$ (R_η) and the lateral width of the shower in the second calorimeter layer (w_2). The sample of electron candidates predominantly consists of: charged hadrons faking electrons, electrons from photon conversions, and prompt electrons (mainly from b,c decays). Small shifts are observed in R_η and w_2 which remain to be understood. Fig. 3 clearly shows that the longitudinal segmentation of the electromagnetic calorimeter can be used to further separate hadrons from true electrons. The fraction of high threshold TRT hits shown in Fig. 3 after application of all other tight cuts highlights the discriminating power of the TRT.

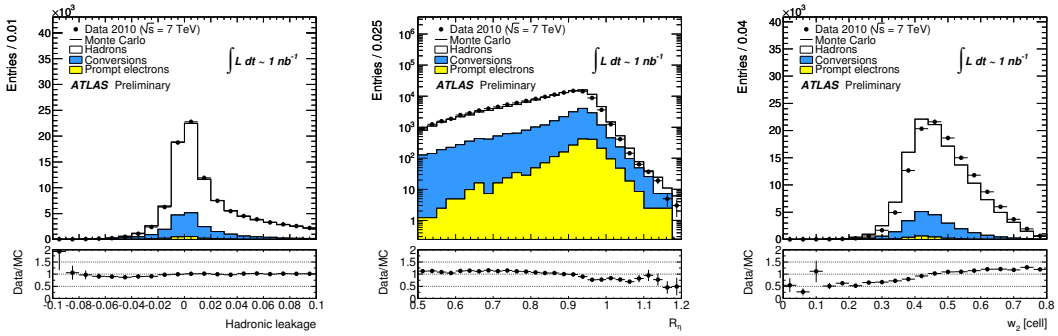

Figure 2: Hadronic leakage (left), R_η (middle) and w_2 (right) at preselection

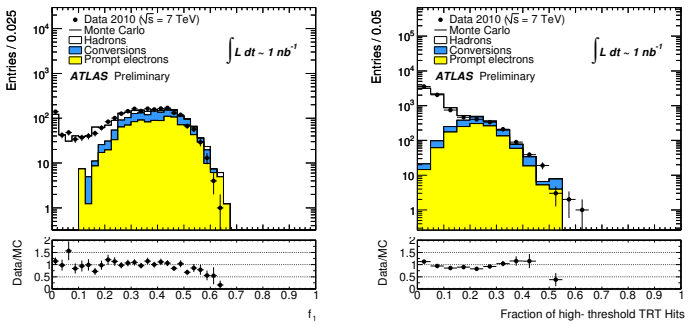

Figure 3: Fraction of energy in the first calorimeter layer, f_1 (left), fraction of high threshold TRT hits (right)

4 J/ψ observation

The J/ψ signal is the first abundant source of isolated electrons from a known resonance to be seen in the ATLAS experiment. Along with the Z boson, it is one of the few "standard candles" that will be used to calibrate the detector and assess the electron performance and identification efficiency. We present here the observation of the J/ψ in the di-electron channel. This has proved challenging in the first few nb^{-1} due to the low p_T spectrum of the J/ψ and the large hadronic background. To improve the reconstruction efficiency at low p_T, the seed finding algorithm of the standard reconstruction is replaced by a topological clustering, which is very effective at identifying low energy deposits above noise and has a very low energy threshold ($E_T > 300$ MeV). The standard fixed size clustering is then seeded from those clusters and a direct comparison with the standard reconstruction is possible. A subset of the variables from the baseline identification are used and the cuts are reoptimised to maximize the signal over the background. In particular, there is a strong reliance on f_1, the lateral shower containment in the η direction, the fraction of high threshold TRT hits and the number of hits in the silicon tracker. This allows us to have a very clean peak with very low background, as can be seen on Fig. 4. The integrated luminosity used is 6.3 nb^{-1} where calorimeter triggered events with an energy deposit greater than 3 GeV are selected. The invariant mass is computed using only track parameters and the track momenta are not corrected for Bremsstrahlung effects. The distribution is fitted with the Novosibirsk [1] function for the signal plus a straight line for the background. The yields extracted from the fit are: 52 ± 8 signal events for 6 ± 4 background events. The fitted mass is (3.05 ± 0.07) GeV which is compatible with the PDG value; the width is (0.27 ± 0.05) GeV.

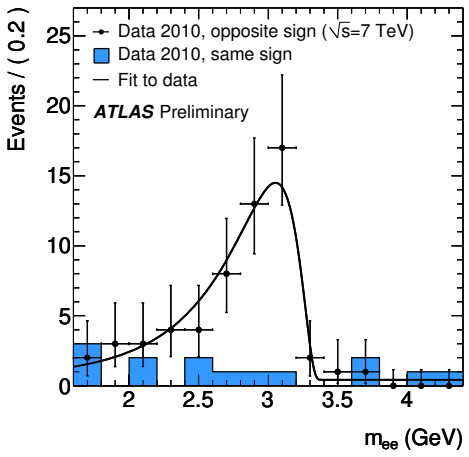

Figure 4: Invariant mass of electron-positron pairs.

[1] The Novosibirsk function is usually defined by: $f(m) = A_S \exp(-0.5\ln^2[1 + \Lambda\tau \cdot (m - m_0)]/\tau^2 + \tau^2)$, where $\Lambda = \sinh(\tau\sqrt{\ln 4})/(\sigma\tau\sqrt{\ln 4})$, the peak position is m_0, the width is σ, and τ is the tail parameter.

5 Conclusion and outlook

The assessment of the electron performance in the ATLAS experiment has started with the study of the first sample of inclusive electrons as well as the observation of the first J/ψ events. In general, their is a good agreement between data and Monte Carlo in the identification variables. Some variables do exhibit a trend which is still to be understood. An essential step towards the measurement of the electron efficiency will be the understanding of the shower shape cuts and track quality requirements commonly used in electron identification. To this effect, a tag-and-probe technique can be used to extract the shower shape and tracking distribution for probe electrons for events in a window around the J/ψ or Z mass. In addition, with the J/ψ and Z boson mass known to high accuracy, the uniformity and energy scale of the electromagnetic calorimeter will be probed and the detector inter-calibrated using the available methods that have been tested over the years in simulation and test-beams. This first look sets the stage for future studies that will benefit from the inreased luminosity expected in the future and provide a direct input to all physics measurements involving electrons.

References

[1] G. Aad *et al.* [ATLAS Collaboration], JINST **3** (2008) S08003.